AGE (2014) 36:21–30
DOI 10.1007/s11357-013-9540-0

Skeletal muscle ATP kinetics are impaired in frail mice

Ashwin Akki · Huanle Yang · Ashish Gupta · Vadappuram P. Chacko · Toshiyuki Yano · Michelle K. Leppo · Charles Steenbergen · Jeremy Walston · Robert G. Weiss

Received: 21 November 2012 / Accepted: 3 May 2013 / Published online: 22 May 2013

Abstract The interleukin-10 knockout mouse ($IL10^{tm/tm}$) has been proposed as a model for human frailty, a geriatric syndrome characterized by skeletal muscle (SM) weakness, because it develops an age-related decline in SM strength compared to control (C57BL/6J) mice. Compromised energy metabolism and energy deprivation appear to play a central role in muscle weakness in metabolic myopathies and muscular dystrophies. Nonetheless, it is not known whether SM energy metabolism is altered in frailty. A combination of in vivo ^{31}P nuclear magnetic resonance experiments and biochemical assays was used to measure high-energy phosphate concentrations, the rate of ATP synthesis via creatine kinase (CK), the primary energy reserve reaction in SM, as well as the unidirectional rates of ATP synthesis from inorganic phosphate (P_i) in hind limb SM of 92-week-old control (n=7) and $IL10^{tm/tm}$ (n=6) mice. SM Phosphocreatine (20.2±2.3 vs. 16.8±2.3 μmol/g, control vs. $IL10^{tm/tm}$, $p<0.05$), ATP flux via CK (5.0±0.9 vs. 3.1±1.1 μmol/g/s, $p<0.01$), ATP synthesis from inorganic phosphate ($P_i \rightarrow ATP$) (0.58±0.3 vs. 0.26±0.2 μmol/g/s, $p<0.05$) and the free energy released from ATP hydrolysis ($\Delta G_{\sim ATP}$) were significantly lower and [P_i] (2.8±1.0 vs. 5.3±2.0 μmol/g, control vs. $IL10^{tm/tm}$, $p<0.05$) markedly higher in $IL10^{tm/tm}$ than in control mice. These observations demonstrate that, despite normal in vitro metabolic enzyme activities, in vivo SM ATP kinetics, high-energy phosphate levels and energy release from ATP hydrolysis are reduced and inorganic phosphate is elevated in a murine model of frailty. These observations do not prove, but are consistent with the premise, that energetic abnormalities may contribute metabolically to SM weakness in this geriatric syndrome.

Keywords Skeletal muscle · Metabolism · ATP · Frailty · Creatine kinase

A. Akki · A. Gupta · M. K. Leppo · R. G. Weiss
Cardiology Division, Department of Medicine, Johns Hopkins University School of Medicine, Baltimore, MD, USA

A. Akki · A. Gupta · V. P. Chacko · R. G. Weiss
Division of Magnetic Resonance Research, Department of Radiology, Johns Hopkins University School of Medicine, Baltimore, MD, USA

H. Yang · J. Walston
Division of Geriatric Medicine and Gerontology, Johns Hopkins University School of Medicine, Baltimore, MD, USA

T. Yano · C. Steenbergen
Department of Pathology, Johns Hopkins University School of Medicine, Baltimore, MD, USA

R. G. Weiss (✉)
The Johns Hopkins Hospital, Blalock 544, 600 N. Wolfe Street, Baltimore, MD 21287-6568, USA
e-mail: rweiss@jhmi.edu

Introduction

Frailty in older adults is a clinical syndrome characterized by skeletal muscle (SM) weakness, increased inflammation and multi-systemic decline; it also is

associated with high risk of adverse health outcomes such as disability and mortality (Walston et al. 2002; Walston et al. 2006). Despite recent advances in frailty research in human cohorts, the mechanisms that mediate SM decline and adverse outcomes in frailty remain unclear (Kanapuru and Ershler 2009). The homozygous interleukin-10 null, B6.129P2-IL10$^{tm/Cgn}$/J (IL10$^{tm/tm}$) mouse has been proposed as a model to study the biology linking chronic inflammation and frailty (Walston et al. 2008) given that they, like frail humans, develop elevated serum interleukin-6 (IL6), muscle weakness, and higher mortality compared to age-matched C57BL/6J (B6) controls (Walston et al. 2008; Ko et al. 2012).

SM uses chemical energy in the form of ATP to fuel the contractile apparatus and other cellular ATPases. Mitochondria play an important role in maintaining adequate ATP supply to the working muscle and preventing muscle fatigue (Russ and Lanza 2011). Compromised energy metabolism and energy deprivation appear to play a central role in muscle fatigability and weakness in metabolic myopathies (Radda 1986; Wortmann 1991; Das et al. 2010) and muscular dystrophies (Radda 1986; Younkin et al. 1987; Barnes et al. 1997) and may underlie SM weakness in frailty (Nair 2005). The creatine kinase (CK) reaction is the primary energy reserve in SM providing ATP during periods of increased demand by rapidly and reversibly converting phosphocreatine (PCr) and adenosine diphosphate (ADP) to ATP and creatine (Cr). SM CK activity is reduced in aging and may contribute to the loss of muscle function (Nuss et al. 2009). Nonetheless, it is not known whether in vivo SM CK energy metabolism is altered in frailty. Given this background, we hypothesized that older, frail IL-10$^{tm/tm}$ mice have reduced SM ATP synthesis and high-energy phosphate (HEP) levels as compared to those of age-matched B6 control mice.

Because in vitro methods to assess cellular energy metabolism such as the measurement of enzyme activities and mitochondrial respiration may not fully reflect the in vivo cellular energy status, ^{31}P magnetic resonance spectroscopy (MRS) was used to measure the in vivo unidirectional rate of ATP synthesis via CK (PCr→ATP) as well as the rate of ATP synthesis from inorganic phosphate (P_i→ATP) in the hind limb SM of 92-week-old IL10$^{tm/tm}$ and age-matched B6 mice to test the hypothesis. We report here that in vivo SM ATP kinetics (both PCr→ATP and P_i→ATP) are markedly depressed in a murine model of frailty suggesting that impaired ATP kinetics, reduced HEP levels and diminished energy release during ATP hydrolysis, as well as increased P_i, are present and could contribute metabolically, in theory, to SM weakness and fatigue in frailty.

Methods

Animals

This investigation conforms to the Guide for the Care and Use of Laboratory Animals published by the US National Institutes of Health (NIH Publication No. 85-23, revised 1996) and was approved by the Institutional Animal Care and Use Committee of the Johns Hopkins University. Ninety-two-week-old male IL-10 deficient (IL10$^{tm/tm}$) and age- and sex-matched C57/BL6 (B6) mice were used for this study. Strength and activity decline with age in IL10$^{tm/tm}$ mice, as compared to control mice, and mortality is increased at this age (Walston et al. 2008; Ko et al. 2012). IL10$^{tm/tm}$ mice were homozygous for the IL10$^{tm/Cgn}$ targeted mutation and were fully backcrossed on B6 background (Kuhn et al. 1993). All mice were purchased from the Jackson laboratory (Bar Harbor, ME; National Institute on Aging, Bethesda, MD) and housed in Johns Hopkins Animal Care facility under specific pathogen-free (SPF) barrier conditions to prevent pathogen contact. Prior to introduction to the barrier, mice were quarantined for at least 1 month and tested to confirm SPF status. The barrier was sentinel tested for a number of pathogens as elaborated in detail previously (Ko et al. 2012). Mice were housed in 75 in.^{2}, autoclave sterilized, high-temperature polycarbonate shoebox cages in ventilated racks (Allentown Inc., Allentown, NJ, USA) containing autoclaved corncob bedding (Harlan Teklad, Indianapolis, IN, USA), autoclaved mouse chow 2018SX (Harlan, Teklad), and reverse osmosis-filtered hyperchlorinated water dispensed through an in-cage automatic watering system (Edstrom Industries, Waterford, WI, USA). Rooms were maintained at 72±2°F on a 14-h light/10-h dark cycle with automated monitoring by Siemens Building Technologies, Inc. (Zurich, Switzerland). Cages were changed every 2 weeks in laminar airflow change stations (The Baker Co., Sanford, ME, USA) with surface cleaning and

disinfection with MB-10 disinfectant (Quip Laboratories Inc., Wilmington, DE, USA). All caging was sanitized by automatic cage washing systems and autoclaved prior to use.

^{31}P MR spectroscopy

Magnetic resonance (MR) experiments were carried out on a Bruker Biospec horizontal bore spectrometer equipped with a 4.7 T/40cm Oxford magnet and a 12 cm actively shielded gradient set, using a custom-built probe assembly as previously described (Gupta et al. 2011). After anesthesia with isoflurane [2 % for induction and 1 % for maintenance] supplied via a nose cone, the mouse was positioned horizontally on the probe platform and the left leg pulled through the ^{1}H coil so as to position the left thigh on a 13 mm ^{31}P surface coil. After the shimming procedure, a scout image was obtained to ensure that only the thigh was situated in the main radio frequency field of the coil. ^{31}P MR spectra were acquired under fully relaxed conditions (90° pulse, 64 scans, and relaxation delay 16 s) using an adiabatic excitation pulse.

Magnetization transfer (MT) was performed to measure the unidirectional rate of ATP synthesis via CK (i.e., CK flux) by applying a continuous wave saturating pulse centered at the γ-ATP for 16 s and measuring the PCr signal intensity (M_0'). A control experiment was performed in which the selective irradiation was placed downfield at a frequency equidistant from the PCr resonance before measuring the PCr signal (M_0). MT experiments were performed to determine the pseudo-first order rate constant ($k_{PCr\rightarrow ATP}$) for the forward CK reaction (PCr+ADP+H^+→ATP+Cr). Intrinsic T_{1PCr}, the relaxation time of PCr in the absence of chemical exchange, calculated in an earlier study in SM from our group was used here to quantify $k_{PCr\rightarrow ATP}$ [$k_{PCr\rightarrow ATP}=(M_0-M_0')/(T_{1PCr}\times M_0')$] (Gupta et al. 2011). CK ATP flux was determined as the product of $k_{PCr\rightarrow ATP}$ and [PCr] (Gupta et al. 2011; Gupta et al. 2012).

MT experiments were also performed to quantify the unidirectional rates of ATP synthesis from P_i in SM. $k_{Pi\rightarrow ATP}$, the pseudo-first order rate constant for P_i→ATP synthesis, was determined by applying a continuous wave saturating pulse centered at the γ-ATP for 16 s and measuring the P_i signal ($M_0'_{Pi}$). This was compared with P_i magnetization in the absence of γ-ATP saturation ($M_{0\ Pi}$). $T1'_{Pi}$, the spin lattice relaxation time for P_i in the presence of γ-ATP saturation measured in an earlier study (Cline et al. 2001), was used here to calculate $k_{Pi\rightarrow ATP}$ [$k_{Pi\rightarrow ATP}=(M_{0\ Pi}-M_0'_{Pi})/(T_1'_{Pi}\times M_{0\ Pi})$]. ATP synthesis from P_i was determined as the product of [P_i] and $k_{Pi\rightarrow ATP}$ (Cline et al. 2001).

Biochemistry

At the end of MR experiments, mice were killed by an intraperitoneal injection of sodium pentobarbital (80 mg/kg body weight and repeated as necessary until a deep level of anesthesia was obtained as documented per toe pinch) and SM from left thigh rapidly frozen in liquid nitrogen. Perchloric acid extracts of SM tissue were obtained (Gupta et al. 2011) and [ATP] measured using a luciferase enzyme based method (Ronner et al. 1999). Subsequently, [PCr] and [P_i] were calculated using MR measured PCr/ATP and PCr/P_i ratios respectively. Creatine was also measured in perchloric acid extracts by an enzyme linked assay (Steenbergen et al. 1977). In vitro, total CK activity was measured in homogenized SM tissue as described previously (Gupta et al. 2011) as was citrate synthase activity using kits from Sigma (C3228 and CS0720) and according to manufacturer's protocol. To determine whether the activity of other major phosphotransfer reactions were altered in the skeletal muscle of frail mice, in vitro activity of hexokinase and adenylate kinase were measured using kits from Biomedical Research Service Center (E-111 for hexokinase) and PromoKine (PK-CA577-K312 for adenylate kinase) and according to manufacturer's protocol. To investigate oxidative stress in muscle tissue, catalase activity was determined using a kit (E-100) from BRSC, University of Buffalo, SUNY and protein carbonylation, a major type of oxidative post-translational modification, was determined with the OxiSelect Protein Carbonyl ELISA kit (STA-310) from Cell Biolabs Inc. SM expression of CK-Muscle isoform (CKM) was determined by standard Western blotting techniques using antibodies specific to CKM as described recently in detail (Gupta et al. 2012).

Serum was separated from blood collected at the time of sacrifice by centrifugation (3,000 rpm for 10 min at 4°C). Serum IL6 levels were measured using

a mouse IL-6 High Sensitivity single-plex ELISA kit from Bioscience (BMS603HS) according to manufacturer's protocol.

Biochemical calculations

Intracellular free [ADP] was calculated from the CK reaction at equilibrium via:

$$[\mathrm{ADP}] = \left([\mathrm{ATP}][\mathrm{free\,CR}] \Big/ ([\mathrm{PCr}][\mathrm{H}^+]K_{\mathrm{eq}}\right) \quad (1)$$

where the cytosolic concentrations are in moles per liter, K_{eq} is 1.66×10^9 L/mol for a $[Mg^{+2}]$ of 1.0 mmol/L (Bittl et al. 1987; Saupe et al. 2000). A cytosolic volume of 0.65 mL/g wet weight (Bittl et al. 1987) was used to convert metabolites measured in millimoles per kilogram wet weight to moles per liter. The free energy change of ATP hydrolysis ($-\Delta G_{\sim\mathrm{ATP}}$ (in kilojoules per mole)) was determined from the formula:

$$\Delta G_{\sim\mathrm{ATP}} = \Delta G_0 + RT\log[\mathrm{ADP}][P_i] \Big/ [\mathrm{ATP}]; \quad (2)$$

where ΔG_0 is the standard free energy change, R the universal gas constant, and T is the absolute temperature (Gibbs 1985).

The theoretically predicted rate of the CK equation was calculated from the following relationship (Bittl et al. 1987):

$$v_f\mathrm{pred} = \left[V_{f\max}[\mathrm{ADP}][\mathrm{PCr}]\right] \Big/ DK_m(\mathrm{ADP})K_i(\mathrm{PCr}) \quad (3)$$

where V_{max} is the reported maximum velocity of the CK reaction (Bittl et al. 1987), [PCr] was measured by ^{31}P MRS as described above, [ADP] was calculated per Eq. [1], the K_m of ADP was 0.15 and K_i of PCr is 4.65, both taken from Bittl et al. (1987), and D was determined from the relationship:

$$\begin{aligned} D = 1 &+ [\mathrm{ADP}] \Big/ K_i(\mathrm{ADP}) + [\mathrm{PCr}] \Big/ K_i(\mathrm{PCr}) \\ &+ [\mathrm{ATP}] \Big/ K_i(\mathrm{ATP}) + [\mathrm{Cr}] \Big/ K_i(\mathrm{Cr}) \\ &+ [\mathrm{ADP}][\mathrm{PCr}] \Big/ K_m(\mathrm{ADP})K_i(\mathrm{PCr}) \\ &+ [\mathrm{ATP}][\mathrm{Cr}] \Big/ K_m(\mathrm{ATP})K_i(Cr) \\ &+ [\mathrm{ADP}][\mathrm{Cr}] \Big/ K_m(\mathrm{ADP})K_i(\mathrm{Cr}) \end{aligned} \quad (4)$$

where the K_m and K_i are as previously reported for skeletal muscle (Bittl et al. 1987), and [ADP], [Cr], [PCr], and [ATP] determined in these studies as described above.

Statistical analysis

Data are expressed as mean±standard deviation (SD). Comparison of two groups was performed with unpaired Student's t test. A value of $p\leq0.05$ was considered statistically significant.

Results

Phenotype

Body weights (31.1±4.7 vs. 34.9±3.7 g, control vs. IL10$^{tm/tm}$, $p=0.14$) were comparable between the two groups. Nonetheless, serum IL6 levels were significantly higher in IL10$^{tm/tm}$ mice (14.8±7.8 pg/ml) compared to those of age-matched controls (3.3±2.6 pg/ml, $p<0.05$).

Skeletal muscle energetics

Mean skeletal muscle [ATP] (6.1±0.5 vs. 6.5±1.0 μmol/g wet weight, IL10$^{tm/tm}$ vs. control, $p=0.35$) and creatine (15.6±3.4 vs. 17.5±2.7 μmol/g wet weight, $p=0.28$) were comparable between the two groups. Figure 1a and b show the representative fully relaxed ^{31}P MR spectra from skeletal muscle of control and IL10$^{tm/tm}$ mice, respectively, at rest. As evident from the spectra, the peak height for PCr was lower while that for P_i higher in IL10$^{tm/tm}$ vs. control mice. This was confirmed by the significantly lower mean [PCr] (16.8±2.3 vs. 20.2±2.3 μmol/g wet weight, IL10$^{tm/tm}$ vs. control, $p<0.05$) and twofold higher mean [P_i] (5.3±2.0 vs. 2.8±1.0 μmol/g, $p<0.05$) in the skeletal muscle of IL10$^{tm/tm}$ mice than those in control mice. Mean calculated cytosolic [ADP] was similar in IL10$^{tm/tm}$ and control mice (64±9 vs. 63±6 μM, $p=0.85$). However, the free energy released with ATP hydrolysis ($\Delta G_{\sim\mathrm{ATP}}$, whereby a more negative number indicates greater energy release) was lower in IL10$^{tm/tm}$ mice (−55.9±1.4 vs. -58.8±1.1 kJ/mol, IL10$^{tm/tm}$ vs. control, $p<0.002$).

Figure 2a and b show the representative skeletal muscle MT spectra from control and IL10$^{tm/tm}$ mice respectively at rest. The reduction in PCr signal intensity with γ-ATP saturated (left vs. right spectrum in

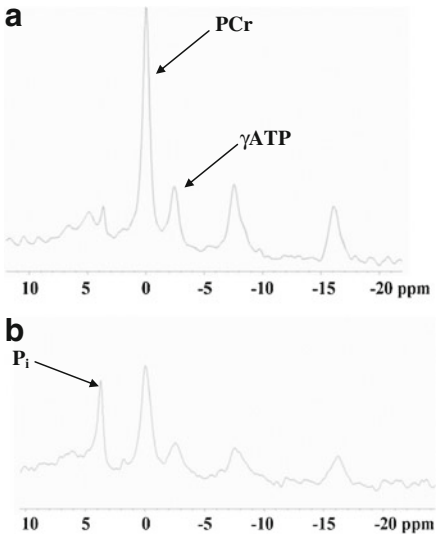

Fig. 1 Fully relaxed ^{31}P MR spectra. Representative fully relaxed ^{31}P MR spectra from the hind limb skeletal muscle of control (**a**) and IL10$^{tm/tm}$ (**b**) mice. Note the substantially higher inorganic phosphate (P_i) signal in the skeletal muscle of IL10$^{tm/tm}$ mouse

each panel) is directly proportional to the rate of ATP synthesis through CK (Weiss et al. 2005). A smaller decline in PCr signal observed in IL10$^{tm/tm}$ vs. control mice indicates lower CK ATP flux in IL10$^{tm/tm}$ mice. The summary values for $k_{PCr\rightarrow ATP}$ (0.18±0.05 vs. 0.25±0.05 s^{-1}, IL10$^{tm/tm}$ vs. control, $p<0.05$) and CK ATP flux (3.1±1.1vs. 5.0±0.9 μmol/g/s, $p<0.01$) were approximately 28 % and 38 % lower, respectively, in IL10$^{tm/tm}$ mice compared to those in controls (Fig. 3).

Mean SM $k_{Pi\rightarrow ATP}$ (0.04±0.02 vs. 0.20±0.05 s^{-1}, IL10$^{tm/tm}$ vs. control, $p<0.0001$) and unidirectional ($P_i\rightarrow$ATP) ATP synthesis rates (0.26±0.2 vs. 0.58±0.3 μmol/g/s, $p<0.05$) were approximately 80% and 55% lower, respectively, in IL10$^{tm/tm}$ mice compared to those in controls (Fig. 3).

In vitro biochemistry

To determine whether the reduction in in vivo ATP synthesis through CK, the primary muscle energy reserve reaction, was due to decreased amounts of CK protein or to maximal CK enzyme activity, in vitro assays were performed on rapidly frozen tissue. SM CKM protein levels were unchanged between control and IL10$^{tm/tm}$ mice (Fig. 4) as were in vitro total CK activity (35.4±2.4 vs.

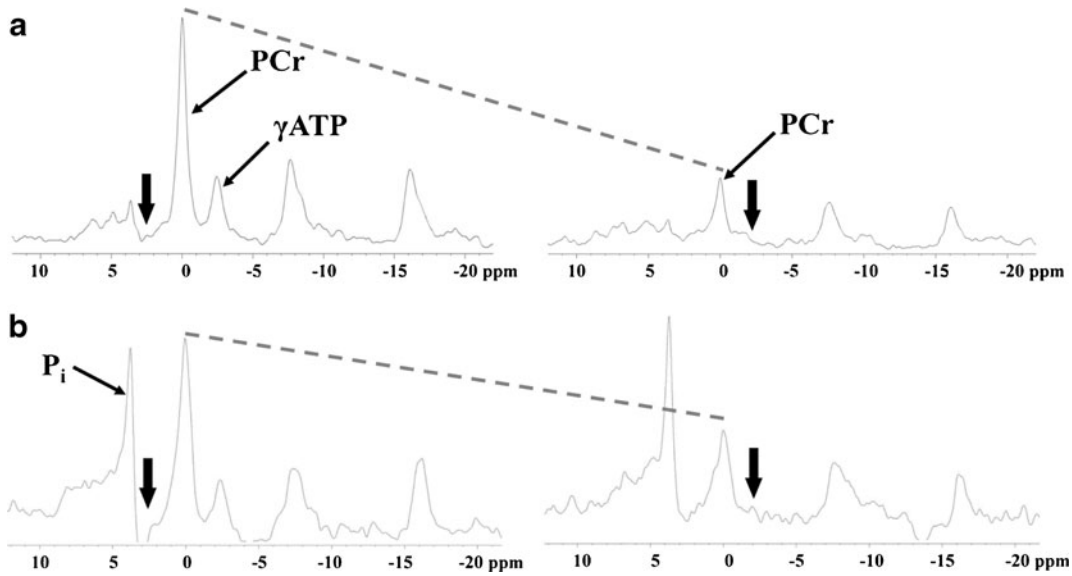

Fig. 2 ^{31}P Magnetization Transfer Spectra. Representative ^{31}P MT spectra from the hind limb skeletal muscle of control (**a**) and IL10$^{tm/tm}$ (**b**) mice. The spectra were acquired with saturating irradiation (*thick arrows*) in the control position (*left spectrum in each panel*) and γ-ATP position (*right spectrum in each panel*). The decrease in the height of PCr peak between control and γ-ATP saturation (*slope of the dotted lines*) is directly related to the rate of ATP synthesis through the CK reaction. A smaller decline in PCr signal with γ-ATP saturation observed in IL10$^{tm/tm}$ vs. control mice indicates lower ATP flux through CK in the skeletal muscle of IL10$^{tm/tm}$ mice

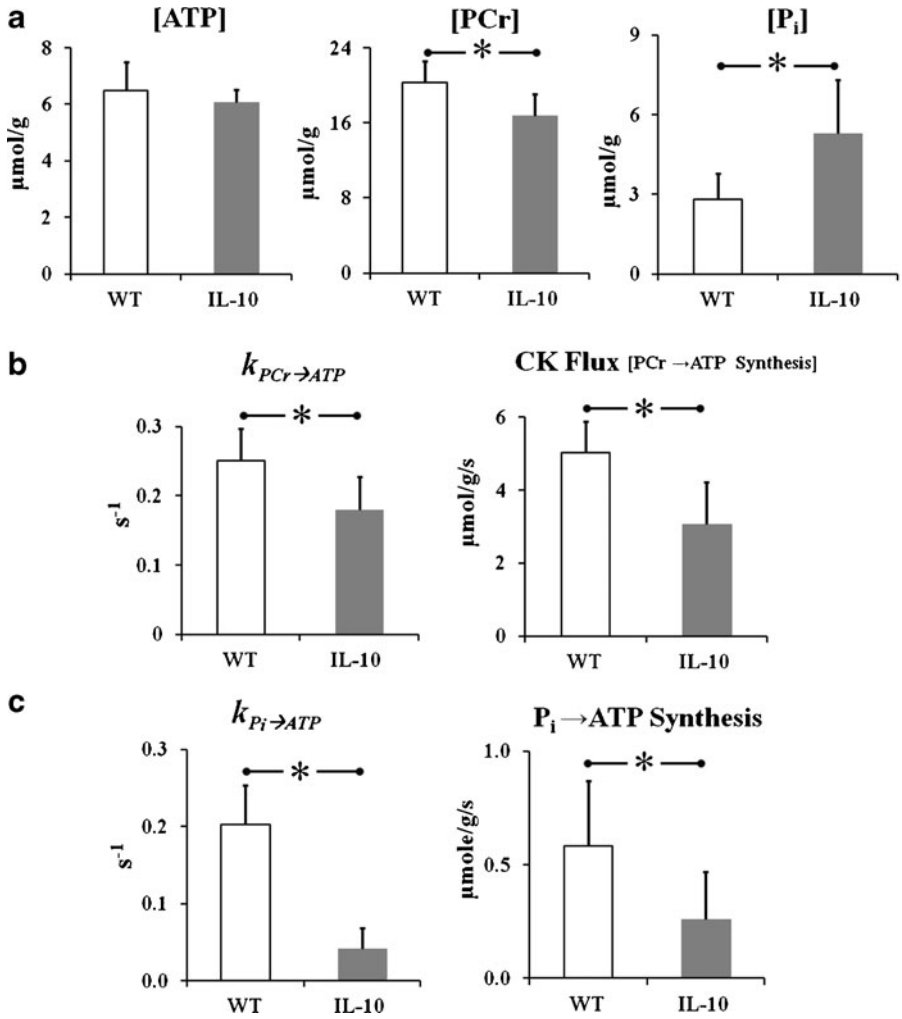

Fig. 3 Skeletal Muscle Energetics. Skeletal muscle concentrations of ATP, Phosphocreatine (PCr) and P_i (**a**), the CK pseudo-first order rate constant ($k_{PCr\rightarrow ATP}$) and rate of ATP synthesis through CK (i.e., CK Flux) (**b**), and the pseudo-first order rate constant for ATP synthesis from P_i ($k_{Pi\rightarrow ATP}$) and unidirectional ($P_i \rightarrow$ ATP) rates of ATP synthesis (**c**) in the hind limb of control (*white bars*) and IL10$^{tm/tm}$ (*gray bars*) mice. The high-energy phosphate, PCr, was lower, P_i was higher and rates of ATP synthesis through both CK and from P_i, were significantly reduced in IL10$^{tm/tm}$ mice as compared to controls. Results are mean±SD for n=6–7 in each group. *p<0.05 vs. control

32.8±2.0 IU/mg protein, IL10$^{tm/tm}$ vs. control, p=0.07, Fig. 4), adenylate kinase activity (6235±1136 vs. 6813±1063 U/mg protein, p=0.37) and hexokinase activity (0.17±0.03 vs. 0.14±0.02 U/mg protein, p=0.26). In vitro SM citrate synthase activity (126.3±24.4 vs. 91.1±28.6 µmol/ml/min/µg protein, IL10$^{tm/tm}$ vs. control, p<0.05) was higher in IL10$^{tm/tm}$ mice than in controls. Thus the in vivo reductions in skeletal muscle ATP delivery rates in IL10$^{tm/tm}$ mice were not associated with decreased CKM expression, CK maximal activity, adenylate kinase/hexokinase activities or mitochondrial citrate synthase activity, suggesting the importance of direct in vivo measures in intact muscle. Catalase activity is commonly increased in conditions with increased oxidative stress and skeletal muscle catalase activity was significantly higher in IL10$^{tm/tm}$ than in control mice (p<0.02, Fig. 5). Protein carbonylation, reportedly the most frequent type of protein modification in response to oxidative stress (England and Cotter 2005), trended higher in IL10$^{tm/tm}$ mice (p=0.06, Fig. 5).

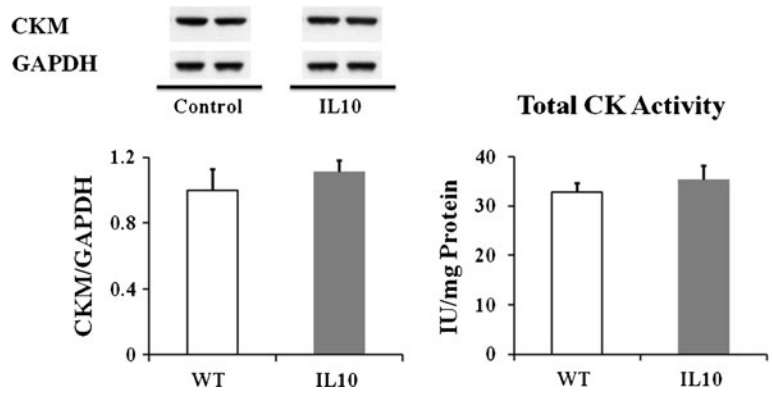

Fig. 4 Skeletal Muscle CK expression and activity. Skeletal muscle CKM protein expression and in vitro total CK activity in control and IL10$^{tm/tm}$ mice. Results expressed as mean±SD for n=6–7 for each group

Discussion

Frailty is characterized by a decline in SM strength and physical activity resulting in adverse outcomes for older adults including disability, institutionalization, and mortality (Marzetti and Leeuwenburgh 2006; Walston et al. 2006; Russ and Lanza 2011). The IL10$^{tm/tm}$ mice develop an age-related increase in SM weakness, inflammation and increased mortality compared to age-matched B6 mice and thus have been proposed as a model of human frailty (Walston et al. 2008; Ko et al. 2012). We report here, for the first time, that in vivo SM energy metabolism is deranged at rest in frail IL10$^{tm/tm}$ mice as evidenced by a decline in intracellular [PCr], accumulation of P_i, together with a decrease in the rate of ATP synthesis via CK (i.e., CK flux) and in the unidirectional rate of ATP synthesis from P_i as compared to age-matched controls. The amount of energy released during ATP hydrolysis is also significantly less in IL10$^{tm/tm}$ mice. These findings demonstrate that, despite normal [ATP] levels, in vivo SM ATP kinetics and utilization are decreased in frailty and represent a metabolic mechanism that could in theory contribute to muscle weakness in this geriatric syndrome.

Mitochondria, which are increasingly thought to influence multiple aging-related disease states including frailty, play a central role in maintaining adequate HEP supply to the working muscle and preventing muscle fatigue with additional energetic support from glycolysis and other phosphotransfer reactions including CK and adenylate kinase (Dzeja and Terzic 2003; Russ and Lanza 2011). As SM energy demand varies by several orders of magnitude from resting to exercise conditions, energy metabolism is tightly regulated in order to meet the widely varying energy requirements (Das et al. 2010). For over two decades, clinical and experimental studies have shown that deranged SM energy metabolism underlies weakness and early fatigability in metabolic myopathies (Radda 1986; Wortmann 1991) and muscular dystrophies (Radda 1986; Das et al. 2010). Further, aging is associated with altered SM energy metabolism (Russ and Lanza 2011) and longitudinal studies have shown that energy availability declines

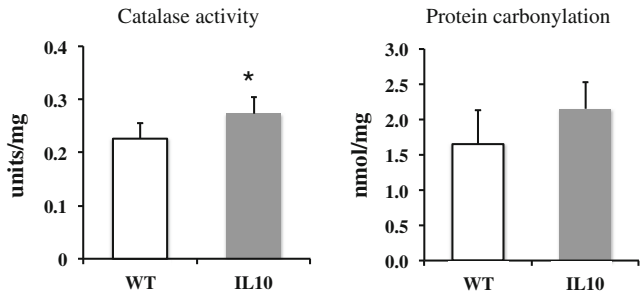

Fig. 5 Skeletal muscle catalase activity and protein carbonylation. Skeletal muscle catalase activity (*left*) and protein carbonylation (*right*) in control ("WT" *white bars*) and IL10$^{tm/tm}$ mice ("IL10", *gray bars*). Catalase activity was significantly higher (*p<0.02) and protein carbonylation trended higher (p=0.06) in IL10 as compared to control hearts. Results expressed as mean ± SD for n=6–7 for each group

and energy needs for independent living increase with aging (Schrack et al. 2010). The results of this study build on those observations and identify specific in vivo SM reductions in ATP production, phosphorylation potential and energy release in frailty.

^{31}P MRS is an excellent tool to noninvasively monitor cellular energy status in vivo by measuring the levels of intracellular phosphorus metabolites namely PCr, ATP and P_i. The technique has been successfully used to elucidate the underlying defect in SM energy metabolism in myopathies with similar clinical presentations (Radda 1986; Wortmann 1991). A unique advantage of ^{31}P MRS is its ability to quantify in vivo kinetics of ATP synthesis from PCr through CK and from P_i. Indeed, in vivo MRS detected significant metabolic abnormalities in the present study that were not detected by in vitro assays of [ATP], CK expression and activity or of enzymatic markers of mitochondrial number. To our knowledge, this is the first study to investigate in vivo SM ATP kinetics in an animal model of frailty.

The unidirectional rates of ATP synthesis from P_i (i.e. $P_i \rightarrow$ATP flux) represent the sum of all ATP synthesis reactions involving P_i through both glycolysis and mitochondrial oxidative phosphorylation (OxPhos), but this is dominated by glyoclytically mediated Pi-ATP exchange (Kemp 2008; Balaban and Koretsky 2011; From and Ugurbil 2011; Kemp and Brindle 2012). An approximately 55% decline in $P_i \rightarrow$ATP flux in IL10$^{tm/tm}$ mice was observed and this lower unidirectional $P_i \rightarrow$ATP flux was not due to substrate driving the reaction since P_i was higher, not lower, in IL10$^{tm/tm}$ mice. The lower $P_i \rightarrow$ATP synthesis could be attributed to a decline in glycolysis, mitochondrial OxPhos, or both. Elevated SM in vitro citrate synthase activity in IL10$^{tm/tm}$ mice argues against a decline in mitochondrial content. Nonetheless, it is possible that mitochondrial enzymes were oxidatively modified (i.e., carbonylation or nitrotyrosine modification) (Feng et al. 2008; Staunton et al. 2011) owing to enhanced inflammation and oxidative stress in IL10$^{tm/tm}$ mice (Ko et al. 2012) which in turn could impair mitochondrial substrate oxidation and/or oxidative phosphorylation. Whatever the reason, the finding of substantially lower SM unidirectional $P_i \rightarrow$ATP synthesis rates in IL10$^{tm/tm}$ mice (vs. control) is novel and not predicted by in vitro measures.

The CK reaction serves as spatial and temporal ATP buffer in SM maintaining high cytosolic [ATP] at sites of ATP utilization and low ADP levels at sites of ATP synthesis (Ventura-Clapier et al. 2004). Both temporal and spatial buffering actions of CK may be important when energy demands vary widely during burst activity in SM (Ventura-Clapier et al. 2004). The ~38 % reduction in CK flux in SM of IL10$^{tm/tm}$ mice could limit ATP supply and/or increase cytosolic free [ADP]. However, [ADP] was unchanged in SM of IL10$^{tm/tm}$ mice. The lower CK ATP flux in IL10$^{tm/tm}$ mice was due to a fall in both $k_{PCr \rightarrow ATP}$ and [PCr] and implies that these mice replenish the ATP pool (assuming no change in oxidative phosphorylation) in approximately twice the time taken by control mice, thereby slowing myofibrillar ATP delivery.

Despite a decline in in vivo skeletal muscle CK ATP flux, CKM protein expression and in vitro total CK activity remained unchanged in IL10$^{tm/tm}$ mice vs. that of age-matched control mice. To gain insight into substrate control of CK, as a possible cause of reduced in vivo CK flux, the forward rate of ATP synthesis through CK was predicted from in vitro metabolite and enzyme activity measures (from Eq. [3]) and compared to direct in vivo CK flux measures, after both were converted to similar units. The measured in vivo CK flux (~7 mM/s) was similar to that predicted (~9.8 mM/s) in control mice, suggesting the enzyme velocity in vivo is mostly under substrate control. However, in IL10$^{tm/tm}$ mice in vivo forward CK flux (~4 mM/s) was much lower than the predicted rate (~10.7 mM/s), suggesting non-substrate regulation in vivo. The ratio of in vivo CK flux to V_{max} reflects how fast the CK reaction is proceeding in vivo relative to its capacity and is influenced by intrinsic properties of the protein, substrate control, and other regulatory factors (Saupe et al. 2000). Further, the mean ratio of in vivo CK flux/CK V_{max} (again after both are converted to common units of mM/s) is 0.066 and 0.036 for control and IL10$^{tm/tm}$, respectively, demonstrating a 45 % reduction of in vivo forward CK flux relative to the maximal CK capacity present in IL10$^{tm/tm}$ mice as compared to that of control mice. Because both of these separate calculations point to non-substrate regulation of CK in skeletal muscle of IL10$^{tm/tm}$ mice, it is tempting to speculate that post-translational modification (i.e., phosphorylation (Ponticos et al. 1998), carbonylation, nitrotyrosine modification, etc.) of CKM protein may occur in frail mice secondary to enhanced oxidative stress, a situation analogous to that observed in SM of aging wild-type mice (Nuss et al. 2009). In support of this

speculation, aged IL10$^{tm/tm}$ mice have increased catalase levels (Fig. 5), suggesting enhanced oxidative stress, and trending higher protein carbonylation (Fig. 5, p=0.06), one of the most common oxidative stress-related post-translational modifications, as compared to age-matched control mice. In contrast, SM $k_{PCr\rightarrow ATP}$ and CK ATP flux in aged control mice (Fig. 3) were comparable to those in young control mice in an earlier study from our group (Gupta et al. 2011). The current and prior data together indicate these differences in frail mice are not due to age alone but inflammation in the setting of advanced age.

Another striking observation in the present study was the markedly higher SM intracellular [P_i] in IL10$^{tm/tm}$ mice (Fig. 3) which could, in part, contribute to SM fatigue and weakness in these mice (Posterino and Fryer 1998). Increased inorganic phosphate reduces myofibrillar Ca^{+2} sensitivity, lessens sarcoplasmic-reticular Ca^{+2} release, and is associated with reduced force production during immobilization in humans (Allen et al. 2008). Increased inorganic phosphate also contributes to reduced energetic efficiency and, importantly, to an unfavorable change in $\Delta G_{\sim ATP}$ (~3 kJ/mol). It cannot be overemphasized that in addition to the significant reductions in the in vivo forward rates of ATP synthesis from both CK and from P_i described above (Fig. 3), for each ATP molecule hydrolyzed there is in addition significantly less free energy generated. Thus, the aged IL10$^{tm/tm}$ mouse model of frailty has multiple deficits in skeletal muscle ATP synthesis and in energy production from ATP hydrolysis that are multiplicative and negatively impact myofibrillar energy availability even at rest.

Limitations

These studies were designed to test for the first time whether or not abnormalities in energy metabolism, associated with weakness in other myopathies (Radda 1986; Wortmann 1991; Das et al. 2010) and muscular dystrophies (Radda 1986; Younkin et al. 1987; Barnes et al. 1997), are present in vivo at rest in aged IL10$^{tm/tm}$ mice. They were not designed to determine whether or not energetic abnormalities cause the muscle weakness that was previously established in this model (Walston et al. 2008). However, now that specific in vivo energetic abnormalities have been identified, these findings can guide future studies, beyond the scope of this investigation, to determine whether interventions that increase unidirectional PCr→ATP through CK, P_i→ATP, or $\Delta G_{\sim ATP}$, alone or in combination, improve muscle function in aged IL10$^{tm/tm}$ mice. Studies of mitochondrial efficiency and uncoupling can now be performed in isolated muscle fibers (Schuh et al. 2012) or in vivo (Conley et al. 2013), and would provide complementary information on bioenergetic decline in this frailty model.

In summary, we show here that in vivo SM energy metabolism particularly that related to CK is reduced in frail IL10$^{tm/tm}$ mice as evidenced by a decline in intracellular [PCr], accumulation of P_i, together with a decrease in the forward rate of ATP synthesis via CK and from P_i. The amount of energy liberated during ATP hydrolysis ($\Delta G_{\sim ATP}$) is also significantly reduced. These findings demonstrate that in vivo SM ATP kinetics and HEP content are reduced in this frail mouse model and may possibly underlie its development of age-related skeletal muscle weakness (Walston et al. 2008). Future studies will also be required in frail human subjects to determine the extent of energetic abnormalities at rest, during activity, and during recovery and to test whether improving intracellular ATP synthesis and/or myofibrillar ATP delivery augments SM performance and strength in frailty.

References

Allen DG, Lamb GD, Westerblad H (2008) Skeletal muscle fatigue: cellular mechanisms. Physiol Rev 88:287–332

Balaban RS, Koretsky AP (2011) Interpretation of 31P NMR saturation transfer experiments: what you can't see might confuse you. Focus on "Standard magnetic resonance-based measurements of the Pi–>ATP rate do not index the rate of oxidative phosphorylation in cardiac and skeletal muscles". Am J of Physiol Cell Physiol 301:C12–15

Barnes PR, Kemp GJ, Taylor DJ, Radda GK (1997) Skeletal muscle metabolism in myotonic dystrophy A 31P magnetic resonance spectroscopy study. Brain : A J of Neurol 120(Pt 10):1699–1711

Bittl JA, DeLayre J, Ingwall JS (1987) Rate equation for creatine kinase predicts the in vivo reaction velocity: 31P NMR surface coil studies in brain, heart, and skeletal muscle of the living rat. Biochemistry 26:6083–6090

Cline GW, Vidal-Puig AJ, Dufour S, Cadman KS, Lowell BB, Shulman GI (2001) In vivo effects of uncoupling protein-3 gene disruption on mitochondrial energy metabolism. J Biol Chem 276:20240–20244

Conley KE, Amara CE, Bajpeyi S, Costford SR, Murray K, Jubrias SA, Arakaki L, Marcinek DJ, Smith SR (2013) Higher mitochondrial respiration and uncoupling with reduced electron transport chain content in vivo in muscle of

sedentary versus active subjects. J Clin Endocrinol Metab 98:129–136
Das AM, Steuerwald U, Illsinger S (2010) Inborn errors of energy metabolism associated with myopathies. J Biomed Biotechnol 2010:340849
Dzeja PP, Terzic A (2003) Phosphotransfer networks and cellular energetics. J Exp Biol 206:2039–2047
England K, Cotter TG (2005) Direct oxidative modifications of signalling proteins in mammalian cells and their effects on apoptosis. Redox Report : Comm in Free Radical Res 10:237–245
Feng J, Xie H, Meany DL, Thompson LV, Arriaga EA, Griffin TJ (2008) Quantitative proteomic profiling of muscle type-dependent and age-dependent protein carbonylation in rat skeletal muscle mitochondria. The J of Gerontol Series A, Biol Sci and Med Sc 63:1137–1152
From AH, Ugurbil K (2011) Standard magnetic resonance-based measurements of the Pi→ATP rate do not index the rate of oxidative phosphorylation in cardiac and skeletal muscles. Am J of Physiol Cell Physiol 301:C1–11
Gibbs C (1985) The cytoplasmic phosphorylation potential. Its possible role in the control of myocardial respiration and cardiac contractility. J Mol Cell Cardiol 17:727–731
Gupta A, Chacko VP, Schar M, Akki A, Weiss RG (2011) Impaired ATP kinetics in failing in vivo mouse heart. Circulation Cardiovascular Imaging 4:42–50
Gupta A, Akki A, Wang Y, Leppo M, Chacko VP, Foster D, Cicares V, Kirk J, Su J, Shi S, Lai S, Paolocci N, Steenbergen C, Gerstenblith G, Weiss RG (2012) Creatine kinase-mediated improvement of function in failing mouse hearts provides causal evidence the failing heart is energy-starved. J Clin Invest 122:291–302
Kanapuru B, Ershler WB (2009) Inflammation, coagulation, and the pathway to frailty. Am J Med 122:605–613
Kemp GJ (2008) The interpretation of abnormal ^{31}P magnetic resonance saturation transfer measurements of Pi/ATP exchange in insulin-resistant skeletal muscle. Am J Physiol Endocrinol Metab 294:E640–642, author reply E643-644
Kemp GJ, Brindle KM (2012) What do magnetic resonance-based measurements of Pi→ATP flux tell us about skeletal muscle metabolism? Diabetes 61:1927–1934
Ko F, Yu Q, Xue QL, Yao W, Brayton C, Yang H, Fedarko N, Walston J (2012) Inflammation and mortality in a frail mouse model. AGE (Dordr) 34:705–715
Kuhn R, Lohler J, Rennick D, Rajewsky K, Muller W (1993) Interleukin-10-deficient mice develop chronic enterocolitis. Cell 75:263–274
Marzetti E, Leeuwenburgh C (2006) Skeletal muscle apoptosis, sarcopenia and frailty at old age. Exp Gerontol 41:1234–1238
Nair KS (2005) Aging muscle. Am J Clin Nutr 81:953–963
Nuss JE, Amaning JK, Bailey CE, DeFord JH, Dimayuga VL, Rabek JP, Papaconstantinou J (2009) Oxidative modification and aggregation of creatine kinase from aged mouse skeletal muscle. Aging 1:557–572
Ponticos M, Lu QL, Morgan JE, Hardie DG, Partridge TA, Carling D (1998) Dual regulation of the AMP-activated protein kinase provides a novel mechanism for the control of creatine kinase in skeletal muscle. EMBO J 17:1688–1699
Posterino GS, Fryer MW (1998) Mechanisms underlying phosphate-induced failure of Ca^{2+} release in single skinned skeletal muscle fibres of the rat. J Physiol 512(Pt 1):97–108
Radda GK (1986) The use of NMR spectroscopy for the understanding of disease. Science 233:640–645
Ronner P, Friel E, Czerniawski K, Frankle S (1999) Luminometric assays of ATP, phosphocreatine, and creatine for estimation of free ADP and free AMP. Anal Biochem 275:208–216
Russ DW, Lanza IR (2011) The impact of old age on skeletal muscle energetics: supply and demand. Current Aging Sci 4:234–247
Saupe KW, Spindler M, Hopkins JC, Shen W, Ingwall JS (2000) Kinetic, thermodynamic, and developmental consequences of deleting creatine kinase isoenzymes from the heart. Reaction kinetics of the creatine kinase isoenzymes in the intact heart. J of Biol Chem 275:19742–19746
Schrack JA, Simonsick EM, Ferrucci L (2010) The energetic pathway to mobility loss: an emerging new framework for longitudinal studies on aging. J Am Geriatr Soc 58(Suppl 2):S329–336
Schuh RA, Jackson KC, Khairallah RJ, Ward CW, Spangenburg EE (2012) Measuring mitochondrial respiration in intact single muscle fibers. Am J Physiol Regul Integr Comp Physiol 302:R712–719
Staunton L, O'Connell K, Ohlendieck K (2011) Proteomic profiling of mitochondrial enzymes during skeletal muscle aging. J of Aging Res 2011:908035
Steenbergen C, Deleeuw G, Rich T, Williamson JR (1977) Effects of acidosis and ischemia on contractility and intracellular pH of rat heart. Circ Res 41:849–858
Ventura-Clapier R, Kaasik A, Veksler V (2004) Structural and functional adaptations of striated muscles to CK deficiency. Mol Cell Biochem 256–257:29–41
Walston J, McBurnie MA, Newman A, Tracy RP, Kop WJ, Hirsch CH, Gottdiener J, Fried LP, Cardiovascular HS (2002) Frailty and activation of the inflammation and coagulation systems with and without clinical comorbidities: results from the Cardiovascular Health Study. Arch Intern Med 162:2333–2341
Walston J, Hadley EC, Ferrucci L, Guralnik JM, Newman AB, Studenski SA, Ershler WB, Harris T, Fried LP (2006) Research agenda for frailty in older adults: toward a better understanding of physiology and etiology: summary from the American Geriatrics Society/National Institute on Aging Research Conference on Frailty in Older Adults. J Am Geriatr Soc 54:991–1001
Walston J, Fedarko N, Yang H, Leng S, Beamer B, Espinoza S, Lipton A, Zheng H, Becker K (2008) The physical and biological characterization of a frail mouse model. J of Gerontol Series A, Biol Sci and Med Sci 63:391–398
Weiss RG, Gerstenblith G, Bottomley PA (2005) ATP flux through creatine kinase in the normal, stressed, and failing human heart. Proc Natl Acad Sci U S A 102:808–813
Wortmann RL (1991) Metabolic myopathies. Curr Opin Rheumatol 3:925–933
Younkin DP, Berman P, Sladky J, Chee C, Bank W, Chance B (1987) ^{31}P NMR studies in Duchenne muscular dystrophy: age-related metabolic changes. Neurology 37:165–169